25th ABCM International Congress of Mechanical Engineering
October 20-25, 2019, Uberlândia, MG, Brazil

COB-2019-0352
FINITE ELEMENT SIMULATION OF STRAIN HETEROGENEITY IN METALS WITH DIFFERENT WORK HARDENING PROPERTIES SUBMITTED TO HPT

Adriano Amâncio Trajano
Marcell Filho da Silva Ferreira
Pedro Henrique Alves Martins
Benedito Carneiro de Andrade Júnior
Universidade Federal de Minas Gerais, Av. Pres. Antônio Carlos 6627, Pampulha, 31270-901, Belo Horizonte, Minas Gerais, Brazil
adriano.a.trajano@gmail.com
eng.marcellferreira@gmail.com
pedromartins.eng@hotmail.com
benedito.andrade40@gmail.com

Abstract. High pressure torsion is one of severe plastic deformation techniques, in which high rates of plastic deformation in the samples are achieved by concurrent application of compressive force and torsional straining. As a result, the exceptional grain refinement is obtained, producing ultrafine-grained materials with excellent mechanical properties, like increased strength and hardness. Such materials can be submitted to superplastic forming in elevated temperatures and used in forging of mechanical components with complex geometries. Depending on the stress states involved in the processing, commonly formed materials exhibit longitudinal and cross-sectional strain heterogeneity. The strain heterogeneity is influenced by work hardening properties of plastically deformed material, being a determining factor in stress and strain distribution in the processed specimens. The aim of the present work is to evaluate this influence in metals with different work hardening rates: AISI 304 stainless steel and Interstitial Free steel, submitted to high pressure torsion. The finite element method was employed in the analysis, and in addition, the effects of the coefficient of friction between the anvils and the specimens, of the strain rate, and of the number of rotations were also assessed. The results demonstrate that the effective deformation of Interstitial Free steel was greater than that of AISI 304 stainless steel. This indicates that in severe plastic deformation processes, like high pressure torsion, the mechanical properties of the metals influence not only the coefficient of friction, but also strain heterogeneity in the samples.

Keywords: *high pressure torsion, strain heterogeneity, stainless steel AISI 304, Interstitial Free steel, work hardening*

1. INTRODUCTION

Material processing using Severe Plastic Deformation (SPD) techniques allows material grain refinement to submicrometer and nanometer sizes (Valiev et al., 1996; Figueiredo and Langdon, 2012). This is achieved by imposing elevated plastic deformation rates on the specimens without any significant changes in the overall dimensions of the workpiece (Zhilyaev and Langdon, 2008). Grain refinement of polycrystalline materials improves mechanical properties of these materials (Zhilyaev and Langdon, 2008; Figueiredo et al., 2011a) and favours their application in superplastic forming methods (Hosford and Caddell, 2007; Kawasaki and Langdon, 2007), attracting, therefore, large scientific interest. Accumulative roll bonding (ARB), equal channel angular pressing (ECAP), and high pressure torsion (HPT) are the most common SPD techniques.

The HPT process was first proposed by Bridgman (1935), and is considered the most effective SPD technique for grain refinement (Calado, 2012). During the HPT processing the disk-shaped metallic sample is placed in a cavity between two steel anvils and is subjected to simultaneous compressive and torsional loading. The resulting hydrostatic pressure prevents the fracture of the specimen and reduces relative slip; high rates of plastic deformation are achieved by rotation of the lower anvil (Larijani et al., 2015).

Figure 1 schematically shows HPT process. Processing of large samples is still a challenging task from a technical point of view (Hohenwarter et al., 2009; Figueiredo and Langdon, 2013), and commonly used specimens are approximately 1,0 mm thick and 10 mm in diameter. Strain heterogeneity is commonly observed in cold-worked materials.

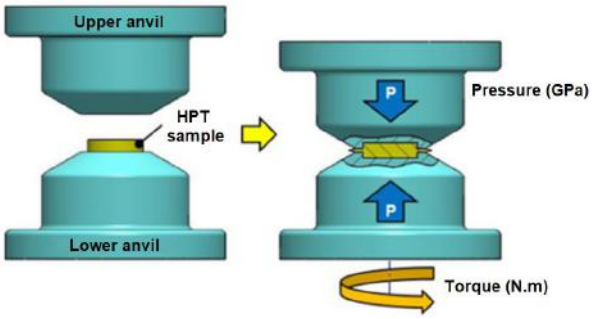

Figure 1. HPT processing scheme (Kawasaki and Langdon, 2007)

The equivalent von Mises strain for HPT processing is given by Figueiredo and Langdon (2013) as:

$$\varepsilon_{vm} = (2\pi Nr)/h\sqrt{3} \quad (1),$$

where ε_{vm} is von Mises equivalent strain in mm/mm, N is the number of rotations applied on the specimen, r is the distance from the centre of the specimen, and h is the thickness of the specimen. It can be seen from the equation that the equivalent strain is directly proportional to the number of applied rotations, and varies along the radius of the specimen, reaching its maximal value when $r=r_{max}$. Thus, it is expected that the strain is heterogeneous along the radius of the specimen, and constant through its thickness. A higher homogeneity of mechanical and microstructural properties along the sample radius is always accompanied by a larger ε_{vm} value (Lee and Kim, 2014).

High plastic deformations in the metals submitted to HPT processing commonly lead to characteristic microstructural transformations. For example, Astafurova et al. (2014) observed in HPT processed AISI stainless steel samples softening, hardening and phase transformation.

Song et al. (2017) reported that the imposed strain caused in HPT processed Interstitial Free (IF) steel samples changes in mechanical properties along the radius of the workpiece, with an increase of hardness and variation of microstructure from the centre to the periphery of the metallic workpiece.

In this context, the aim of the present study is to use finite element modelling to analyse the strain heterogeneity of HPT processed metals with different mechanical properties.

2. MATERIALS AND METHODS

Prior to the finite element method (FEM) analysis, the samples of AISI 304 stainless steel and IF steel were submitted to the tensile tests to obtain the characteristic stress-strain curves of materials in annealing state. The obtained curves were then added to the database of the software used for computational analysis to ensure the reliability of simulation results.

FEM simulations of HPT processing of two materials with different work hardening rates (AISI 304 stainless steel and IF steel) were performed using DEFORM 2D/3D software (Scientific Forming Technologies Corporation, Columbus, OH, USA). In the simulations, the geometry of the two anvils was considered equal, and the specimens were modelled as 8 mm thick disks, 10 mm in diameter. The upper anvil was used to apply the compressive force, whilst the lower anvil applied the constant torsion at 1 rpm. Both anvils had a 10 mm diameter cavity for placing the specimen, with depth less than half the thickness of the disk. In this quasi-constrained HPT configuration the anvils do not touch each other during the processing, and the material can partially flow between them, allowing application of higher hydrostatic pressure on the samples (Figueiredo et al., 2011b).

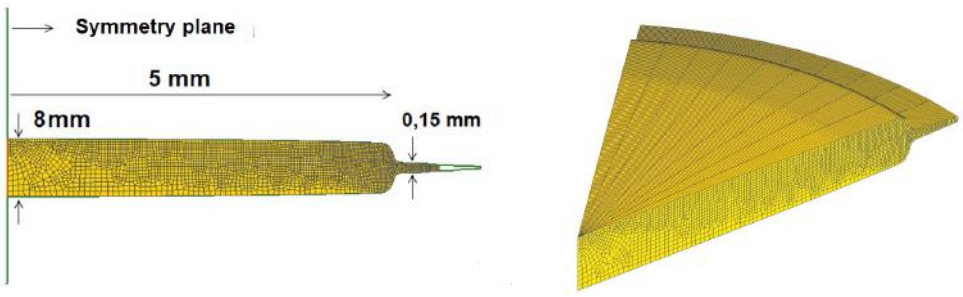

(a) (b)

Figure 2. Sample dimensions used in simulations (a) and a partial 3D view of the sample (b)

The samples were modelled as plastic objects, and the anvils were considered rigid bodies. The used 2D mesh consisted of 20000 elements with mesh refinement on the upper anvil. A sticking condition was adopted between the sample and anvil cavity top and bottom surfaces. Figure 2 shows the geometry of the sample used in the simulations, in a partial 2D and 3D view. The samples are symmetric, therefore only a half of the samples are needed to be modelled (Fig. 2(a)), and then the symmetry considerations were used to produce the complete 3D geometry. Figure 2(b) shows a partial 3D model of the sample. The use of a symmetric 2D partial model increased the simulation speed, optimizing the testing time.

High compressive loads are expected on the top of the samples, therefore, a non-uniform mesh, denser on the top of the samples, was chosen. The upper and lower anvils were tested under distinct conditions: the upper anvil was considered under a hybrid friction of the static friction and shear friction with the sample (since besides the friction depending on the pressure load, the upper anvil also receives a reaction to the shear force applied by the lower anvil); the lower anvil was considered in shear friction condition.

First, the HPT processing simulations were performed at different numbers of rotation N =1/2 (180^o) and N = 1 (360^o), constant coefficient of friction (C_f) between the walls of the cavities and the sample equal to 1.5 and pressure P = 1 GPa, for both materials. After the simulations, the effective strain was measured from the centre of the samples to the point of the highest strain.

After that, the simulations were performed with different coefficients of friction C_f = 1, C_f = 1.5 and C_f = 2 at the contact regions between the samples and the upper and lower anvils. The other parameters were kept constant, including the number of rotations (N = 1) and pressure (P = 1 GPa). After the simulations with different coefficients of friction, the effective strain was measured from the centre of the samples to the point of the highest strain. The coefficients for the simulation were chosen based on the information available in the literature; according to the available data, the variation in the strain heterogeneity becomes significant starting from C_f = 1,0. The strain heterogeneity for both materials after HPT simulations with different coefficients of friction it will also be graphically compared.

Finally, aiming to analyse the strain heterogeneity in HPT simulation increasing pressure, the loads of 78 540 N and 392 700 N, corresponding to pressures of 1 and 5 GPa, respectively, from the upper anvil, was simulated at N = 1/2 and N = 1. After the simulations, the effective strain was measured from the centre of the samples to the point of the highest strain. The strain heterogeneity for both materials after HPT simulations with different coefficients of friction it will also be graphically compared.

3. RESULTS AND DISCUSSION

Figure 3 shows experimentally obtained stress-strain curves for AISI 304 stainless steel and IF steel in annealing state.

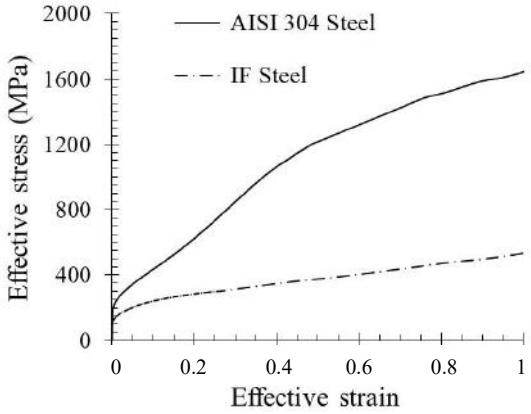

Figure 3. Stress-strain curves of AISI 304 and IF steel

The yield points obtained in the tensile tests of the metals are in agreement with data found in the literature (Shojaati and Beidokhti, 2017; Máthins and Krajnak, 2011).

Figure 4 shows the effective strain values of AISI 304 and IF steel samples after HPT; the values are measured from the centre to the edge of the samples, for (a) N = 1/2 and (b) N = 1, at C_f = 1 and P = 1 GPa. It was observed that the effective strain of the HPT processed disks increased with the increase of N, indicating that strain heterogeneity tends to intensify with the increase of the number of rotation; the result found also by Wei et al. (2013) and Song et al. (2014).

It was also observed that IF steel deformed more than AISI 304 steel; this behaviour became more prominent at higher N.

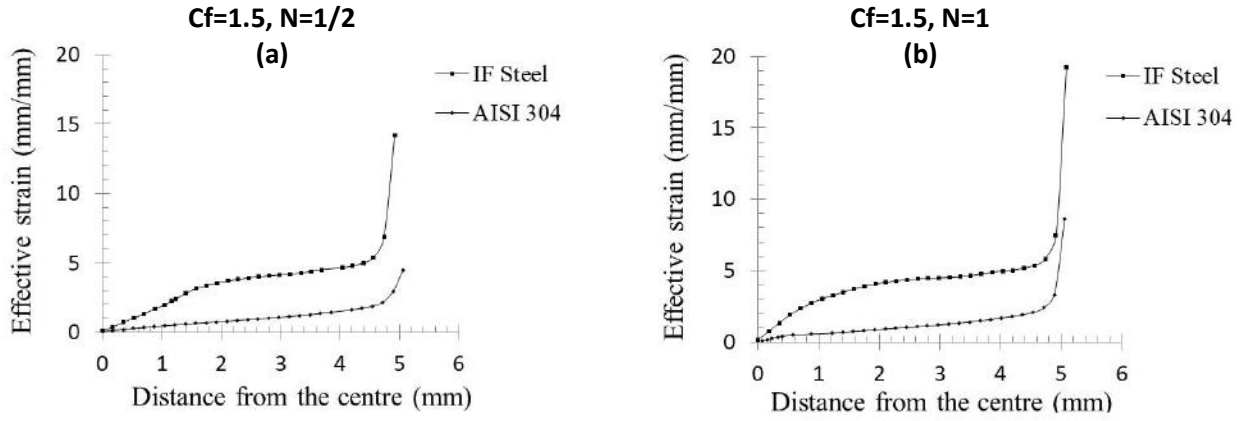

Figure 4. Effective strain as a function of the distance from the centre of the disk for AISI 304 and IF steel after HPT (a) N = 1/2 (b) N = 1

Figure 5 shows the effective strain distribution in HPT processed AISI 304 and IF steel samples for the coefficient of friction C_f=1.5, pressure P = 1 GPa and number of rotations N = 1, in a partial 3D view of the simulated samples. To compare the strain heterogeneity of the effective strain from the centre of the sample to its periphery, a comparative deformation scale up to 10 mm/mm was used; higher strains in the samples were not considered.

Figure 6 shows the effective strain distribution in HPT processed AISI 304 and IF steel samples for the coefficient of friction C_f=2, pressure P = 1 GPa and number of rotations N = 1, in a partial 3D view of the simulated samples. To compare the strain heterogeneity of the effective strain from the centre of the sample to its periphery, a comparative deformation scale up to 30 mm/mm was used; higher strains in the samples were not considered.

In IF steel and AISI 304 steel samples, a non-homogeneous effective strain distribution in radial direction was observed, with higher strain values at the edges of the samples. It can be seen from Fig. 5 and Fig. 6 that IF steel shows greater strain than AISI 304 steel. Despite of change of the coefficient of friction (C_f=1.5 and C_f=2), non-homogeneous effective strain distribution keep increased for IF Steel compared with AISI 304, with high values of effective strain coefficient of friction C_f=2. This indicates that mechanical and microstructural aspects responsible for the differences in the stress-strain curves and plastic deformation of IF steel and AISI 304 steel samples influence also the HPT test results (Zhilyaev and Langdon, 2008; Figueiredo et al., 2011b). This heterogeneity of deformation tends to increase as the number of revolutions increases (Song et al., 2014).

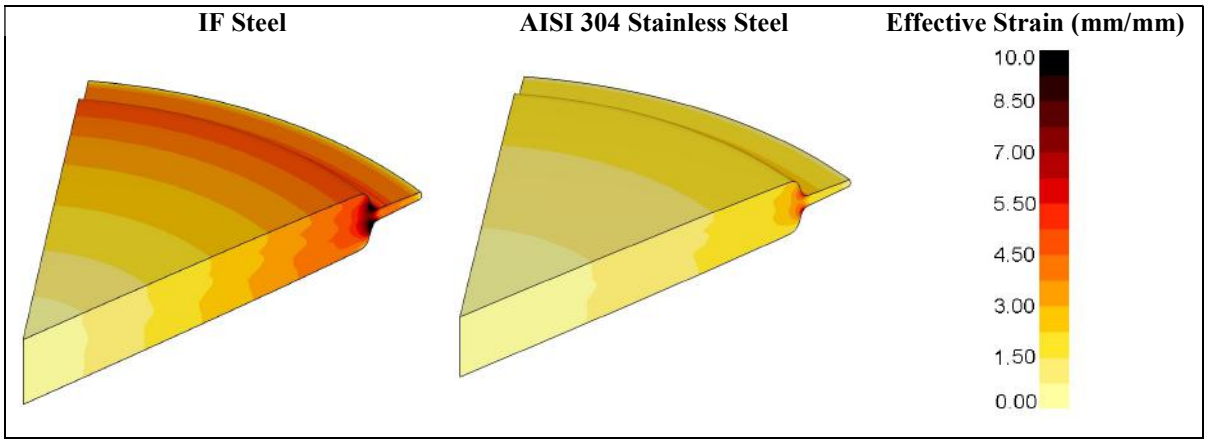

Figure 5. Effective strain distribution in IF and AISI 304 steel samples after HPT, partial 3D view (C_f=1.5, P = 1 GPa, N = 1)

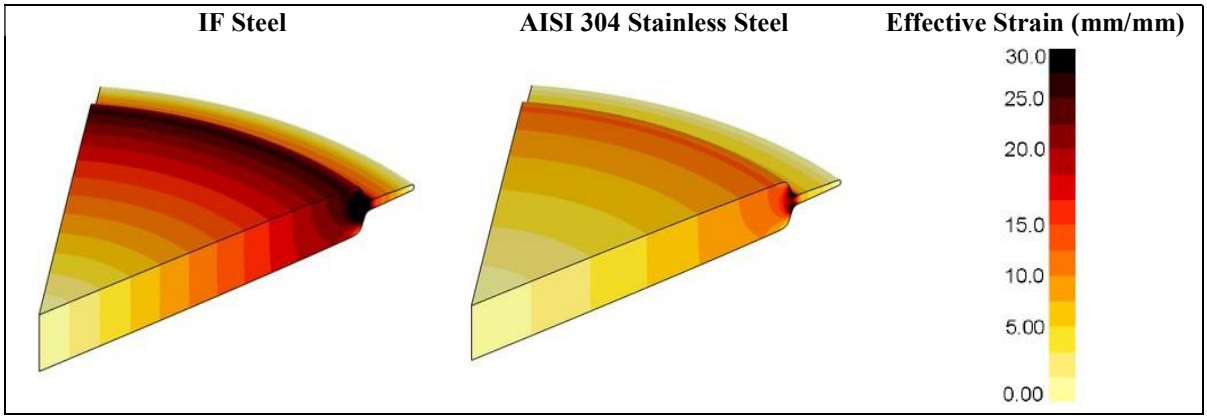

Figure 6. Effective strain distribution in IF and AISI 304 steel samples after HPT, partial 3D view (C_f= 2, P = 1 GPa, N = 1)

Figure 7 shows the effective strain curves as a function of the distance from the centre of the disk after HPT processing simulations with different coefficients of friction between the samples and the anvils (C_f = 1, C_f = 1.5 and C_f = 2), at N = 1 and P = 1 GPa, for AISI 304 and IF steel samples. The effective strain is measured from the point of the smallest to the point of the highest effective strain; highest effective strains for AISI 304 and IF steel samples were now considered.

Though the effective strain values in the central part of the samples are similar for both coefficients of friction, farther from the centre the effective strain was significantly greater at C_f = 2 than at C_f = 1; this increase in the effective strain was greater for IF steel (Fig. 7(a)) than for AISI 304 stainless steel (Fig. 7(b)). The observed effect of coefficient of friction for both materials is in agreement with the results found in other studies of the effect of friction on HPT processing (Lee and Kim, 2014).

In the medial and peripheral regions of the samples, the shear forces caused by the coefficient of friction were high enough to reach the sticking condition between the samples and the anvil surfaces.

These results suggest that the friction force (i.e. the coefficient of friction) would affect the effective stress more in the medial and peripheral regions of the sample than in the central part. Thus, the shear friction stress, responsible for the condition of almost bonding between the surfaces, tends to increase with the increase in the number of rotations of the sample.

With the adopted hybrid shear and normal friction (that tend to increase the friction as the pressure increases), higher coefficients of friction tend to increase the strain, especially near the edge (Song et al., 2014). Under the same conditions, the effective strain caused by the coefficient of friction will equally influence both samples, therefore IF steel will have a greater deformation due to its low work hardening rate.

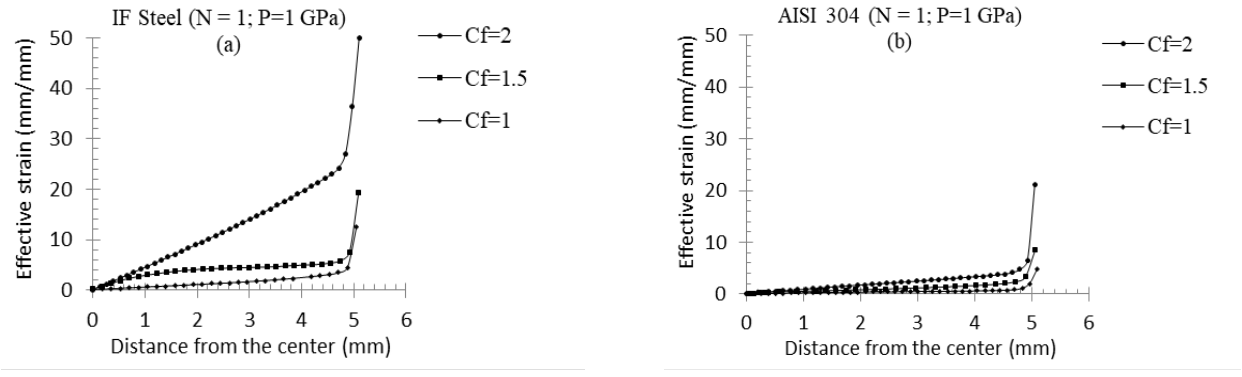

Figure 7. Effective strain as a function of the distance from the centre of the disk after HPT (a) IF steel (b) AISI 304 stainless steel

Figure 8 shows the effective strain distribution in HPT processed AISI 304 and IF steel samples, for the coefficient of friction C_f=1.5, P = 5 GPa and number of rotations N = 1, in a partial 3D view of the simulated samples. To compare the strain heterogeneity of the effective strain from the centre of the sample to its periphery, a comparative deformation scale up to 50 mm/mm was used; highest effective strains of the samples were not considered.

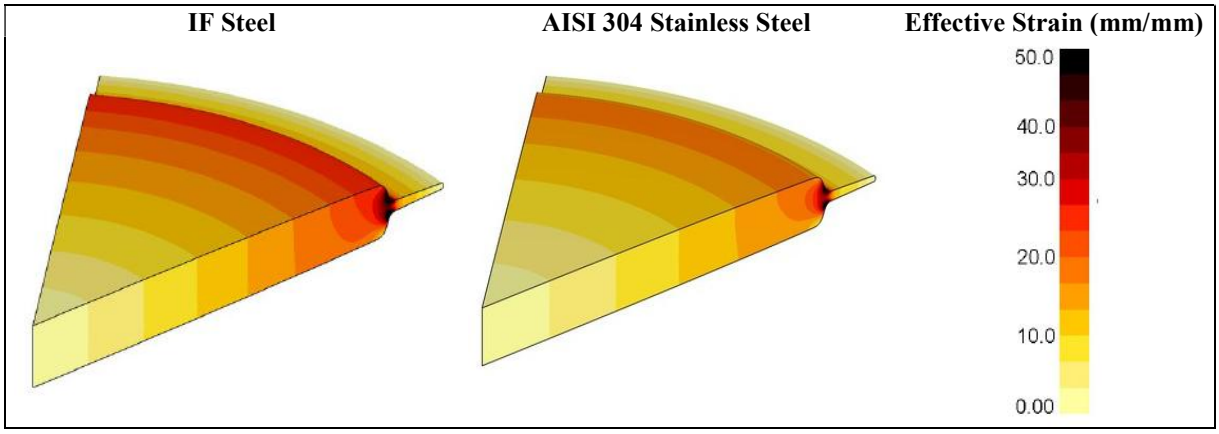

Figure 8. Effective strain distribution in IF and AISI 304 steel samples after HPT, partial 3D view (C_f=1.5, P = 5 GPa, N = 1)

Though the strain values were significantly greater, mainly due to increase of the pressure in HPT test, the observed strain heterogeneity from the centre to the edge of the sample was similar for both samples. This indicates that the influence of pressure on strain heterogeneity in the tested materials is not significant.

Figure 9 shows the effective strain distribution in HPT processed AISI 304 and IF steel samples, for the coefficient of friction C_f=1.5 and P = 5 GPa. The values are measured from the lowest to the highest effective strain point. No significant difference in strain was found between the tested samples. This can be explained by the increased normal load that restricts the effect of the shear friction stress, which has a major influence on the deformation in the torsional phase (Song et al., 2014).

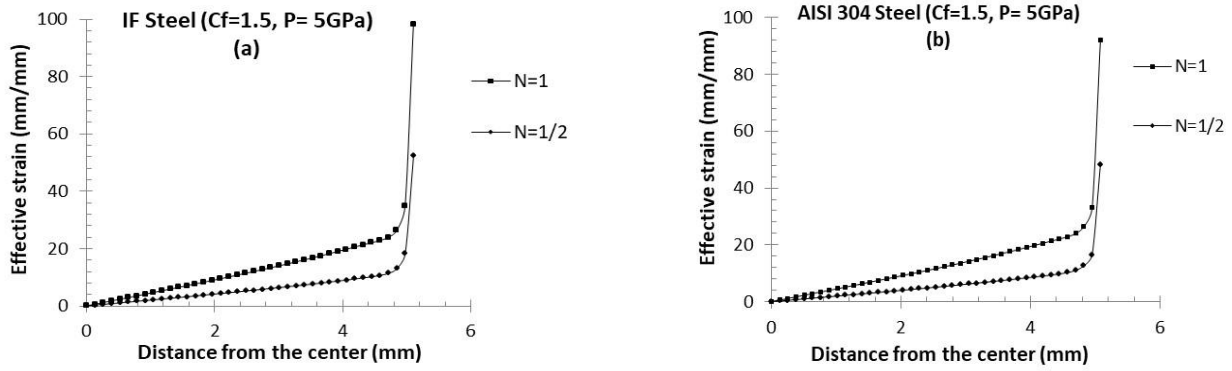

Figure 9. Effective strain as a function of the distance from the centre of the disk after HPT (a) IF steel (b) AISI 304 steel

Although there was no significant difference between the effective deformation for P = 5 GPa, variations in the torque behavior required to rotate the lower anvil as a function of the time, in both samples, was observed, as shown in Figure 10. It was observed, in both samples, the torque increases continuously with time and, therefore, with the increased angle of rotation (Figueiredo et al., 2011b).

This increase is due to the strain hardening, different work hardening properties of both samples and the increase in radius increases the momentum of rotation of the samples, so a larger torque is required. It is also observed that a higher torque was required to rotate the AISI 304 sample than of the IF Steel sample, indicating that even in high load simulations the mechanical properties, related to the materials, mostly with different work hardening properties are sensitive to severe deformation processes.

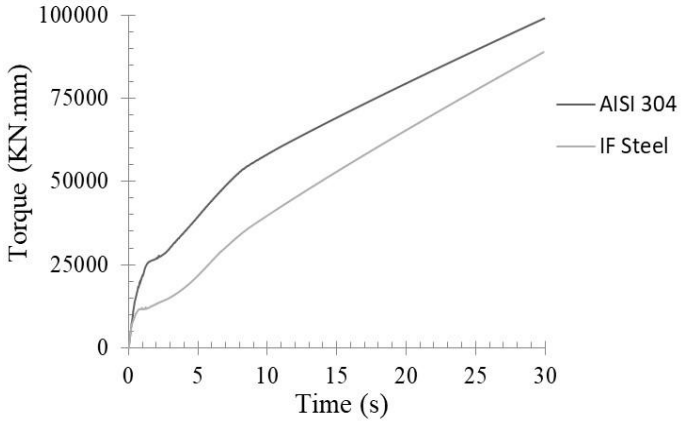

Fig. 10. The estimated torque required to rotate the lower anvil as a function of the time, for coefficient of friction C_f=1.5 and P = 5 GPa.

4. CONCLUSIONS

1 – FEM simulation revealed a high strain heterogeneity in HPT processed samples; this heterogeneity increases with the increase of number of rotations, friction and load, both for AISI 304 stainless steel and IF steel samples.

2 – Under the same simulation conditions, the strain heterogeneity and effective strain of IF steel was significantly greater than of AISI 304 stainless steel, indicating that the mechanical properties of the tested metals, especially work hardening properties, influence the results of severe plastic deformation.

3 – An increase in friction between the samples and the anvils results in an increase of the effective strain that causes increase in strain heterogeneity in the tested samples, as well as higher effective strain of IF steel in comparison to AISI 304 stainless steel.

4 – The increased load caused higher effective strain values in the samples, however, there was no significant difference in these values between two tested materials; strain heterogeneity in this case also did not differ between the samples of IF steel and AISI 304 stainless steel,

5 – It was observed that a higher torque was required to rotate the AISI 304 sample to the IF Steel sample, indicating that even in high load simulations the mechanical properties related to the materials are sensitive to severe deformation processes.

5. ACKNOWLEDGEMENTS

The authors gratefully acknowledge the important financial support of FAPEMIG, CAPES and CNPq for realization of this work.

6. REFERENCES

Astafurova, E., Tukeeva, M.S., Maier, G. and Melnikov, E.V., 2014. "Microstructure and mechanical response of single-crystalline high-manganese austenitic steels under HPT: The effect of stacking-fault energy". *Materials Science and Engineering: A*, Vol. 604, pp. 166–175.

Bridgman, P.W., 1935. "Effects of high shearing stress combined with high hydrostatic pressure". *Physical Review*, Vol. 48, pp. 825–847.

Calado, W.R., 2012. *Ultra-refino de Grão através de Deformação Plástica Severa por Ensaios de Torção*. Ph.D., thesis. Universidade Federal de Minas Gerais, Belo Horizonte, Brasil.

Figueiredo, R., Kawasaki, M. and Langdon, T., 2011a. "An evaluation of homogeneity and heterogeneity in metals processed by HPT". In *Proceedings of the 12th International Symposium on Physics of Materials*. Prague, Czech Republic.

Figueiredo, R., Cetlin, P. and Langdon, T., 2011b. "Using finite element modeling to examine the flow processes in quasi-constrained HPT". *Materials Science and Engineering: A*, Vol. 528, pp 819–820.

Figueiredo, R. and Langdon, T., 2012. "Fabricating ultrafine-grained materials through the application of severe plastic deformation: a review of developments in Brazil*". Journal of Materials Research and Technology*, Vol. 1, pp 55–62.

Figueiredo, R. and Langdon, T., 2013. "Heterogeneous flow during high-pressure torsion". *Materials Research*, Vol. 16(3), pp. 571–576.

Hohenwarter, A., Bachmaier, A., Gludovatz, B., Scheriau, S. and Pippan, R., 2009. "Technical parameters affecting grain refinement by high pressure torsion". *International Journal of Materials Research*, Vol. 100, No. 12, pp. 1653–1661.

Hosford, W.F. and Caddell, R.M., 2007. *Metal Forming: Mechanics and Metallurgy*. Cambridge University Press, New York, 3^{d} edition.

Kawasaki, M. and Langdon, T., 2007. "Principles of superplasticity in ultrafine-grained materials". *Journal of Materials Science*, Vol. 42, pp. 1782–1796.

Larijani, N., Kammerhoferb, C. and Agnus Ekha, M., 2015. "Simulation of high pressure torsion tests of pearlitic steel". *Journal of Materials Processing*, Vol. 22, pp. 337–343.

Lee, D.J. and Kim, H. S., 2014. "Finite element analysis for the geometry effect on strain inhomogeneity during high-pressure torsion". *Journal of Materials Science*, Vol. 49, pp. 6620–6628.

Máthins, K. and Krajnak, T., 2011. "Structure and mechanical behavior of IF steel processed by ECAP". *Journal of Alloys and Compounds*, Vol. 509, pp. 3522–3525.

Shojaati, M. and Beidokhti, B., 2017. "Characterization of AISI 304/AISI 409 stainless steel joints using different filler materials". *Construction and Building Materials*, Vol. 147, pp. 608–615.

Song, Y., Wang, W., Gao, B., Yoo, D., Lee, D. and Kim, H., 2014. "Finite Element Analysis of the Effect of Friction in High Pressure Torsion". *Metals and Materials International*, Vol. 20, pp. 445–450.

Song, Y., Chen, M., Wang, W. and Gao, B., 2017. "Inhomogeneous deformation of interstitial free steel during the HPT process". *Korean Journal of Metals and Materials*, Vol. 55, pp.710–715.

Valiev, R., Ivanisenko, Y., Rauch, E. and Baudelet, B., 1996. "Structure and deformation behavior of Armco iron subjected to severe plastic deformation". *Acta Materialia*, Vol. 44, pp. 4705–4712.

Wei, P., Lu, C., Tieu, K., Deng, G., Wang, H. and Kong, N., 2013. "Finite element analysis of high pressure torsion". *Steel Research International*, Vol. 84, No. 12, pp. 1246–1251.

Zhilyaev, A.P. and Langdon, T.G., 2008. "Using high-pressure torsion for metal processing: fundamentals and applications". *Progress in Materials Science*, Vol. 53, pp. 893–979.

7. RESPONSIBILITY NOTICE

The authors are the only responsible for the printed material included in this paper.